A SMALL-SIGNAL ANALYSIS OF THE ELECTRON CYCLOTRON BACKWARD-WAVE OSCILLATOR

By
K. K. Chow and R. H. Pantell

Technical Report
for
National Science Foundation
Grant 15011

M. L. Report No. 851
October 1961

Microwave Laboratory
W. W. Hansen Laboratories of Physics
Stanford University
Stanford, California

A SMALL-SIGNAL ANALYSIS OF THE ELECTRON CYCLOTRON BACKWARD-WAVE OSCILLATOR

By

K. K. Chow and R. H. Pantell

Technical Report
for
National Science Foundation
Grant 15011

M. L. Report No. 851

October 1961

Microwave Laboratory
W. W. Hansen Laboratories of Physics
Stanford University
Stanford, California

SUMMARY

The construction and performance of the electron cyclotron backward-wave oscillator for operation in the S-band region were reported by the authors last year.[1] It was shown that in an unloaded waveguide supporting the dominant mode, an electron having transverse rotation at its cyclotron frequency would remain in the same rf phase for a relatively long time if the rf frequency were approximately equal to the cyclotron frequency. Furthermore, the transverse electron motion would interact with the rf H-fields giving rise to longitudinal bunching. A hollow beam, after bunching, would have the appearance of a rotating helix with the energy in the transverse electron motion delivered to the rf circuit. In this paper a small signal analysis is presented and the device is examined in the light of that analysis.

The method used in this treatment is the normal-mode expansion type of analysis.[2,3] The electromagnetic field existing in the circuit in the presence of rf current is expanded as a double infinite series of normal modes, out of which only one mode is in approximate dc synchronism with the beam and contributes to cumulative interaction. The rf current is computed from the equation of electron motion under the dc and rf fields. Combination of the circuit equation with the rf current equation leads to the solution of the propagation constants of the waves. This contains six roots; two of them, being very far from synchronism, are not considered for the normal operation of this tube. The remaining four consist of three backward waves and one forward circuit wave; of the three backward waves, two are recognized as being originated from the backward fast cyclotron wave, and one is from the backward circuit wave. Start-oscillation conditions can be calculated from a knowledge of these propagation constants. The theoretical start-oscillation current is found to depend critically on the reflection coefficient at the electron gun end. Proper adjustment of this parameter leads to excellent agreement between the theoretical and experimental results. The rf space-charge forces are neglected in the above analysis.

TABLE OF CONTENTS

LIST OF FIGURES

I. BRIEF DESCRIPTION OF THE OSCILLATOR AND EXPERIMENTAL RESULTS

The oscillator, together with a solenoid is shown diagrammatically in Fig. 1(a). It is constructed from standard, rectangular copper S-band waveguides with a hollow electron beam injected from one end down the waveguide axis. The solenoid, placed over the interaction section of the tube, produces a uniform magnetic field in the axial direction as shown in Fig. 1(b). The hollow electron beam passes through the anode annulus, where a radial magnetic field is excited, into the region of uniform longitudinal dc magnetic field. The electrons will rotate at the cyclotron frequency corresponding to the longitudinal dc magnetic field and interact with the rf fields in the waveguide system at approximately this frequency. With proper adjustment, backward-wave oscillation is obtained with a frequency continuously tunable over the range 2.1 to 3.9 kMc/s. Power output is found to increase steadily from the high frequency end, being at the highest (about 16 watts) at 6 kv beam voltage near the cutoff frequency of the dominant waveguide mode. Efficiency is also found to increase in approximately the same fashion.

Harmonic power contents were found to be low, with the second harmonic about 60 db below the fundamental. Start-oscillation current increased almost linearly with frequency varying from 4 ma at the low frequency end to about 40 ma at the high frequency end. As a backward-wave amplifier, its bandwidth is extremely narrow, being constant at about 7 Mc/s and centered at the cyclotron frequency range, corresponding to about .2 per cent bandwidth.

II. DC ELECTRON MOTION AND CIRCUIT EQUATION

Using an injection scheme as discussed in Section I makes it impossible to obtain exact solutions to the dc electron motion. However, it can be seen that each electron will rotate at the cyclotron frequency around a flux-line to give many small electron beams rotating in parallel. If the original beam is small in diameter and is injected axially into a waveguide supporting the dominant mode, then all the small beams are rotating in a region where the fields are uniform. Hence, in the following analysis we shall consider a small beam rotating around the waveguide

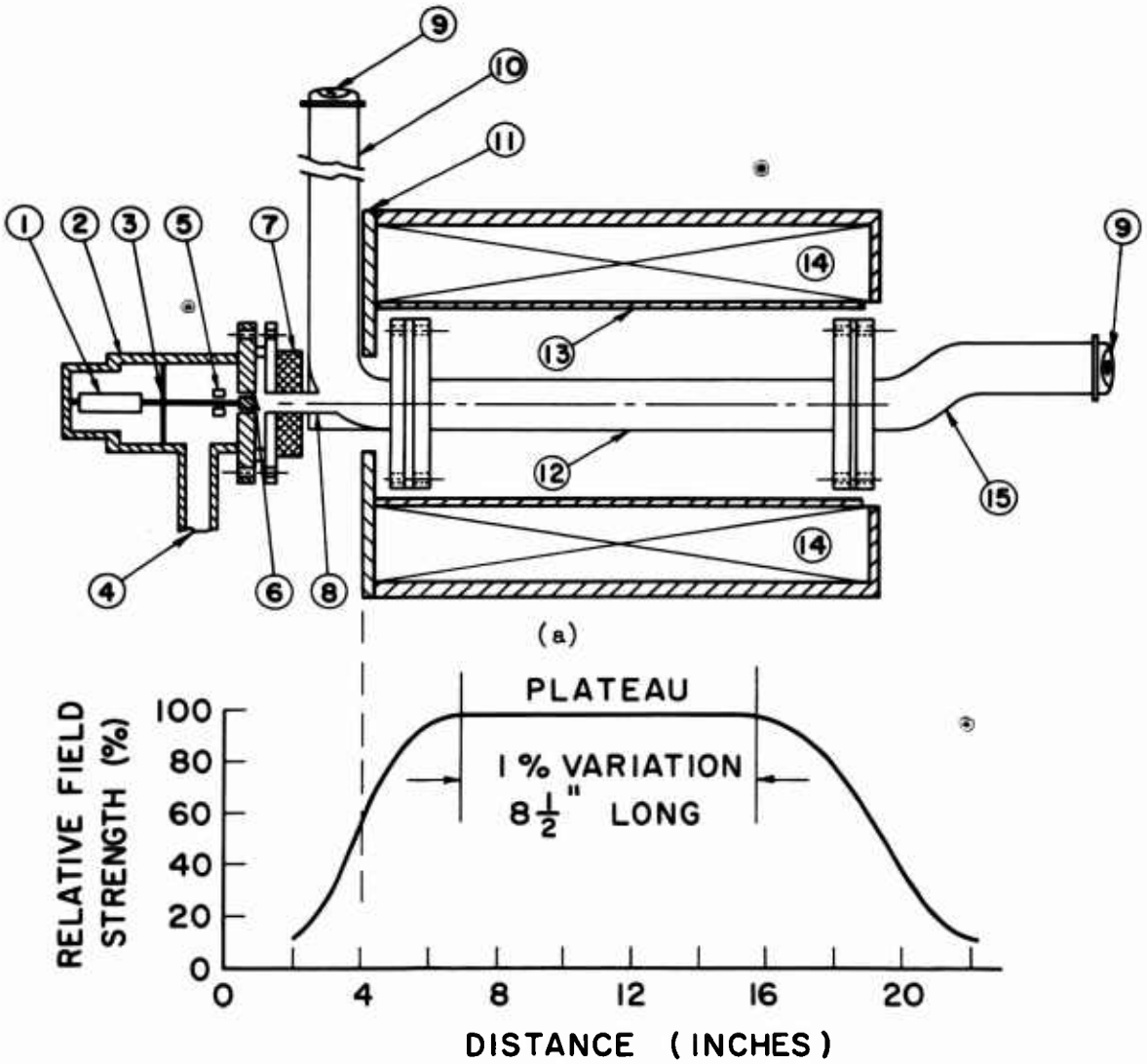

FIG. 1--(a) Cross-sectional view of the essential parts of the oscillator: (1) auxiliary coil, (2) hollow beam gun assembly, (3) vacuum deal, (4) pump-out tube, (5) cathode, (6) anode annulus with radial magnetic field for turning the beam, (7) neck coil, (8) neck, (9) Kovar glass window, (10) waveguide output, (11) soft iron magnetic shield, (12) interaction section, (13) compensation coils, (14) main solenoid, internally cooled, (15) collector section.

(b) Main magnetic field-strength distribution.

axis and interacting with the fields there. The effects of other parallel beams are directly additive and are taken into account by increasing the dc current of this small beam to the total current in the waveguide.

In the presence of the rf currents, the electromagnetic fields propagating in a waveguide can be written as a summation of normal modes. Each of the normal modes has a longitudinal propagation constant Γ_n associated with it and can be resolved into circularly polarized components with field variations p ranging from $-\infty$ to $+\infty$. For TE fields in a rectangular waveguide near the guide-axis, we obtain the following circuit equation, the derivation of which has been given elsewhere:[2,3,4]

$$E_{1T} = \sum_{p,n} \frac{\Gamma_n [\int (J_{1r} E_{rpn} - J_{1\phi} E_{\phi pn}) e^{jp\phi}\, dA] \vec{E}_{Tpn}\, e^{-jp\phi}}{(\Gamma_n^2 - \Gamma^2) 2P_{pn}} , \qquad (1)$$

where the subscript 1 indicates[1] total rf quantities; the subscripts T, r, ϕ indicate components in transverse, radial and azimuthal directions, respectively; subscript p indicates the azimuthal variation of fields of a normal mode and n indicates a particular normal mode of longitudinal propagation constant Γ_n; dA is an element of the beam cross-sectional area; E is the electric field; J is the rf current density; and P is the power associated with a normal mode.

It is readily seen from Eq. (1) that beam-circuit interaction takes place between the transverse components. This is to be expected as there is no E-field in the z-direction.

III. SYNCHRONISM CONDITION AND HARMONIC POWER CONTENTS

It has been shown[1] that "exact dc synchronism" between the electron beam and the qm^{th} mode is defined by the following equation:

$$\omega = \frac{q\phi_0}{1 \pm (\dot{z}_0 / v_m)} , \qquad (2)$$

---

[1] This notation of subscripts will be used throughout this analysis, unless otherwise stated. An additional subscript z indicating the longitudinal component will be used later.

where $\dot{\phi}_0$ is the cyclotron frequency of the electrons, $\dot{z}_0$ is the dc longitudinal velocity of the electrons, and v_m is the phase velocity of the m^{th} normal mode. Therefore with low velocity electrons, ω is almost equal to $q\dot{\phi}_0$. Thus for a given frequency, there is only one azimuthal field configuration that is synchronous; this will be designated as the q^{th} mode. This equation shows the sources of all the higher harmonics: for if interaction is with the lowest order mode, $q = 1$, then the output frequency, ω_1, is approximately the electron cyclotron frequency, $\dot{\phi}_0$, as obtained before. If, however, we have $q = 2$, then ω_2 is approximately $2\dot{\phi}_0$, and so on.

Harmonic generation due to this type of interaction is necessarily weak because the fields of the higher order modes approach zero near the guide axis where the beam is situated. Another possible source of higher harmonic interaction is from an electron rotating at $\dot{\phi}_0$ in the nonuniform part of the dominant mode of frequency near $q\dot{\phi}_0$. Again, it is seen that the output through this interaction is weak since the strong dc magnetic field confines electrons to the region of essentially uniform rf field.

By rearranging Eq. (2) in the following form,

$$\omega = \pm \beta_m \dot{z}_0 \pm q\dot{\phi}_0 , \qquad (3)$$

where β_m is the phase constant corresponding to v_m, we can plot the Brillouin diagram as seen along the z-axis. Figure 2 is such a diagram: the parabola is the waveguide dispersion curve, the straight lines represent beam waves with positive β_m and q [2] (in this case $q = +1$) but with different $\dot{\phi}_0$'s.

From Fig. 2 it is seen that when the operation point $\dot{\phi}_0'$ is far from the cutoff point of the mode, the separation between the backward-wave and forward-wave operation frequencies is relatively large, as given by the vertical distance between the intercepts. As the operation frequency approaches cutoff, frequency separation gradually disappears and interference between the forward and backward wave occurs. That is to say, energy transfers from the forward-wave interaction to the backward wave and vice-versa. Such an interference is not necessarily undesirable, for

---

[2] Negative q will not give cumulative interaction; the interaction due to negative β_m can also be represented by that due to positive β_m.

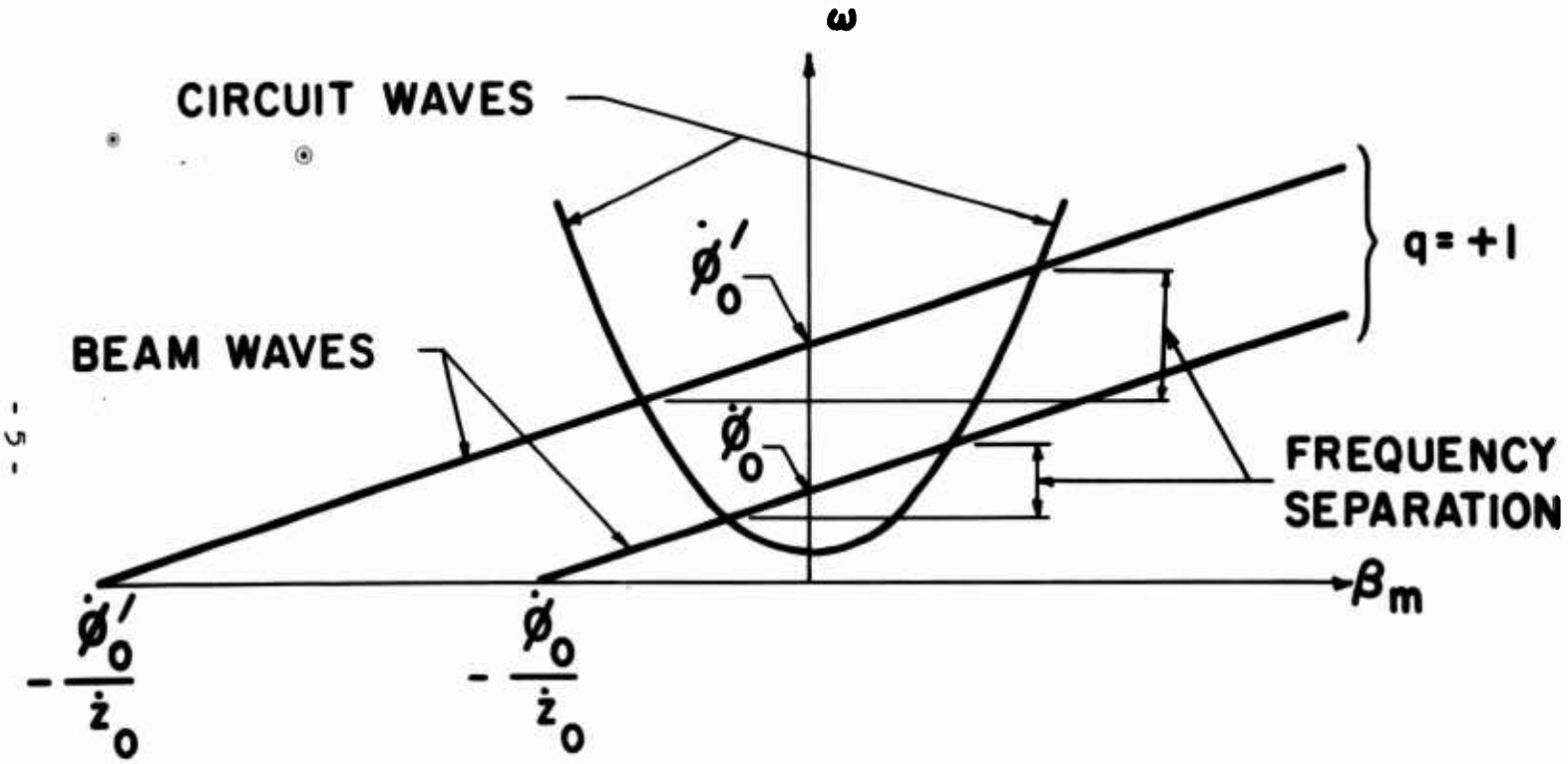

FIG. 2--Brillouin diagram for the circuit and beam waves as seen along the z-axis. The hyperbola corresponds to circuit waves and straight lines correspond to beam waves. The frequency separation between forward-wave and backward-wave interaction points at different operation frequencies is apparent.

if the phase of the forward wave and that of the backward wave can be so arranged that they interfere constructively, i.e., if they aid in electron bunching and energy extraction, then an increase in power output and efficiency will result. This explains the boosting of output power and efficiency observed in the tube with tunable forward load at low frequencies. Tuning of the load alters the amount of reflection from the forward end so as to give constructive interference; thus, the best output does not occur at well-matched points but at off-matched points, as was observed experimentally.

IV. SOLUTIONS OF THE PROPAGATION CONSTANT

In the presence of the circuit fields J_1 must have the same z dependence as the circuit fields, $e^{-\Gamma z}$, and can be resolved in terms of normal modes. The synchronous mode, as has been found, will have azimuthal field variations as $e^{-jq\phi}$. Hence, in the following, these two dependencies will be understood.

The rf current density is given by the expression[5]

$$\vec{J}_1 = \rho_0 \frac{\partial \vec{S}_1}{\partial t} + \nabla \wedge (\rho_0 \vec{S}_1 \wedge \vec{v}_0) \ , \tag{4}$$

where ρ_0 = dc charge density,

$\vec{v}_0$ = dc electron velocity, and

$\vec{S}_1$ = perturbed charge position, i.e., the first-order displacement of the charges which, in the absence of rf excitation, will be at the dc position $\vec{S}_0$.

By expressing Eq. (4) in terms of rf velocities and displacements, and then by substituting into Eq. (1) with thin beam assumptions, we find, after some simplification, that

$$\vec{E}_{1T} = \sum_n \frac{\vec{E}_{Tqn}\, e^{-jq\phi}\, \Gamma_n}{(\Gamma_n^2 - \Gamma^2) 2P_{qn}} \left(- \frac{I_0}{\dot{z}_0} \right)$$

$$\times \left\{ \dot{r}_1 E_{rqn0} - r_0 E_{\phi qn0} [\dot{\phi}_1 + \dot{\phi}_0 (\Gamma z_1 + jq\phi_1)] \right.$$

$$\left. - r_1 \dot{\phi}_0 (E_{\phi qn0} + r_0 E'_{\phi qn0}) \right\} \ , \tag{5}$$

where I_0 is the dc beam current; $\dot{r}_1$ and $\dot{\phi}_1$ are the rf radial and azimuthal electron velocities, respectively; E_{rqn0} and $E_{\phi qn0}$ are the radial and azimuthal fields of the qn^{th} mode at the mean radius of the beam, respectively; and

$$E'_{\phi qn0} = \frac{d}{dr}\,(E_{\phi qn})\Big|_{r=r_0} .$$

The first term in the bracket in Eq. (5) arises from the interaction between rf radial current and field. The rest arise from the interaction between rf azimuthal current and field; viz., the second term is a part of azimuthal current due to rf angular motion; the third term and the fourth term are due to longitudinal and azimuthal bunching. The last two terms are due to radial displacement of the beam in a region in which variation of the quantity rE_ϕ is present.(3)

The expressions for rf electron velocities and displacements can be obtained by considering the electron motion under the influence of the total rf fields of the waveguide and the dc magnetic field of the solenoid. For the case of a thin electron beam, these expressions can be much simplified and substitution of them into Eq. (5) yields

$$E_{1T} = \sum_n \frac{\vec{E}_{Tqn}\, e^{-jq\phi}\, \Gamma_n}{(\Gamma_n^2 - \Gamma^2)2P_{qn}} \left(-\frac{I_0}{\dot{z}_0}\right) \frac{1}{W^2(W^2 + \dot{\phi}_0^2)}\, F , \qquad (6)$$

where W is the quantity $(j\omega - jq\dot{\phi}_0 - \Gamma\dot{z}_0)$ and F is a function of W, total rf waveguide fields, dc beam radius and dc electron velocities.

We are interested only in the synchronous mode, designated as the m^{th}, for which $\Gamma_m \approx \Gamma$. The above summation may then be reduced to one term, viz., when $n = m$, and $\vec{E}_{1T} \approx \vec{E}_{Tqm}\, e^{-jq\phi}$.

Near synchronism, we have $\Gamma \approx \Gamma_m = j\beta_m$ and $\omega - q\dot{\phi}_0 - \beta_m\dot{z}_0 \approx 0$. Therefore, we find $W = j\omega - jq\dot{\phi}_0 - \Gamma\dot{z}_0 \approx 0$, and $W^2 + \dot{\phi}_0^2 \approx \dot{\phi}_0^2$. As a result, Eq. (6) reduces to

$$1 = \frac{\Gamma_m}{(\Gamma_m^2 - \Gamma^2)2P_{qm}} \left(-\frac{I_0}{\dot{z}_0}\right) \frac{\eta E^2_{\phi qm0}}{\dot{z}_0^2 W^2} \left\{[jq\alpha - (\gamma + 1)]W - r_0^2\dot{\phi}_0^2\Gamma\mu_0\gamma_{qm}\right\} \qquad (7)$$

---

(3) For the derivation of these terms, see Appendix A, Reference 4.

where

$$\alpha = \frac{E_{rq}}{E_{\phi q}},$$

$$\gamma = r_0 \frac{E'_{\phi qmO}}{E_{\phi qmO}},$$

μ_0 = permeability of free space and

$$Y_{qm} = -\frac{H_{rqm}}{E_{\phi qm}}.$$

The first term in the bracket in Eq. (7) contains the factor W, and it therefore represents a small but finite contribution to the interaction. It consists of two parts: (i) The $jq\alpha$ part, arising from the dominant component of the $\partial\phi_1/\partial\phi$ term in $J_{1\phi}$, is the azimuthal bunching term resulting from interaction between the longitudinal dc magnetic field and rf radial motion of the electrons. (ii) The $-(\gamma + 1)$ part, arising from the $\partial\rho_0/\partial r$ terms of $J_{1\phi}$ is the result of interaction between dc azimuthal current and the spatially varying rf E-fields.[4] The second term arises from the $\partial z_1/\partial z$ term in $J_{1\phi}$, that is, the interaction due to longitudinal bunching, which, in turn, arises from the transverse rf H-field interacting with the angular motion of the electrons as was predicted from physical considerations. The factor Y_{qm} approaches zero near cutoff, and hence this term is dominant at frequencies away from cutoff. In other words, all the terms arise from the $J_{1\phi}$ component of the rf current, and not from any other component. This can be physically understood because thatpower extraction is obtained through interaction with transverse E-field as was mentioned earlier. It can also be seen from Eq. (7) that the higher the transverse velocity the more efficient the interaction.

For a tube to operate as a backward-wave oscillator, interaction of the bunched beam has to be with a normal mode having a group velocity in the negative z-direction, and hence the sign of P_{qm} in Eq. (7) has to

---

[4] See Appendix A, Reference 4.

be reversed. For the dominant mode, $q = 1$, and in the region of the beam, the rf fields and derivatives may be assumed to vary as Bessel functions and their derivatives. Therefore we have $\alpha \to j$ and $\gamma \to 0$. Furthermore, the propagation constants may be written as

$$\Gamma_m = -j\beta = -\frac{jq\dot{\phi}_0}{\dot{z}_0} + j\beta_e + j\beta_e Cb - \beta_e Cd = -\frac{j\dot{\phi}_0}{\dot{z}_0} + j\beta_e + j\beta_e Cb - \beta_e Cd$$

$$\Gamma = -\frac{jq\dot{\phi}_0}{\dot{z}_0} + j\beta_e - \beta_e C\delta = -j\beta - j\beta_e Cb + \beta_e Cd - \beta_e C\delta ,$$

where we have assumed $q = 1$ and used Pierce's[6] notation, i.e.,

C = gain parameter, much less than unity,

b = velocity parameter, taking into account the slippage between the beam harmonic and the wave velocities,

d = loss parameter, taking the circuit losses into account,

δ = incremental propagation constant,

β = circuit wave phase constant = $(\omega/c)\zeta$,

β_e = electron phase constant = $\omega/\dot{z}_0$ and

$\zeta \triangleq \sqrt{1 - (\text{cutoff frequency/operating frequency})^2}$.

After substituting the above into Eq. (7), we finally obtain a quartic in δ, indicating four roots:

$$\delta^2 = \frac{j\left\{\dfrac{2Cc^2}{r^2\dot{\phi}_0^2\zeta^2}\delta + j\left[1 - \dfrac{\beta_e C}{\beta}(j\delta - b - jd)\right]\right\}}{\left[1 - \dfrac{\beta_e C}{2\beta}(j\delta - b - jd)\right](j\delta - b - jd)C^3}\left\{\frac{\zeta^2 r_0^2\dot{\phi}_0^2}{c^2}\frac{\eta I_0 E_{\phi lm0}^2}{4\omega^2 P_{lm}}\right\} . \quad (8)$$

Actually, the solution contains six waves, because Eq. (6) contains the sixth power of δ (two in Γ^2, two in W^2, another two in $W^2 + \dot{\phi}_0^2$). By neglecting W^2 in $W^2 + \dot{\phi}_0^2$, we have neglected two waves which are very much out of synchronism. The remaining four waves are identified as two circuit waves, $(\Gamma_m^2 - \Gamma^2 \to 0)$ and two fast cyclotron waves $(W^2 \to 0)$.

By neglecting the waveguide losses which are negligible and by defining

$$C^3 = \frac{\zeta^2 r_0^2 \dot{\phi}_0^2 \eta I_0 E_{\phi 1m0}^2}{4\omega^2 c^2 P_{1m}} \triangleq \frac{\zeta^2 r_0^2 \dot{\phi}_0^2}{c^2}\left(\frac{\beta}{\beta_e}\right)^2 \frac{I_0}{4V_0} K ,$$

where $V_0 \triangleq \dot{z}_0^2/2\eta$ = effective beam potential for longitudinal motion,

$K \triangleq E_{\phi 1m0}^2/2P_{1m}\beta^2$ = interaction impedance,

we can rearrange Eq. (8) as follows:

$$\frac{\beta_e C}{2\beta}\delta^4 + j\left(1 + \frac{\beta_e C b}{\beta}\right)\delta^3 - b\left(1 + \frac{\beta_e C b}{2\beta}\right)\delta^2 - j\left(\frac{2Cc^2}{r_0^2\dot{\phi}_0^2\zeta^2} + \frac{\beta_e C}{\beta}\right)\delta + \left(1 + \frac{\beta_e C}{\beta}\right) = 0 . \qquad (9)$$

If the parameters $(2Cc^2)/(r_0^2\dot{\phi}_0^2\zeta^2)$ and $(\beta_e C)/\beta$ can be neglected, Eq. (9) reduces to the same equation as given by Johnson[7] for the O-type BWO. But, from our experimental measurements, these parameters are not negligible, and so we shall solve Eq. (9) using a Burroughs 220 computer and experimentally measured β , β_e , C , etc., for various assumed values of b .

The solutions show that at start-oscillation there are three backward waves, one unattenuated, one growing and one attenuating, and an unattenuated forward wave. These four waves represent the most general situation after the two nonsynchronous waves are neglected; they are identified as two unattenuated circuit waves, one in the same direction as and one in the opposite direction to that of the electron stream, and two backward cyclotron waves, one growing and one attenuating in the direction opposite to that of the electron flow.

V. START-OSCILLATION CONDITIONS AND BACKWARD-WAVE GAIN

For the determination of start-oscillation conditions two possible boundary conditions may be imposed: (i) the forward wave is negligible, and so there are only three backward waves, (ii) all the four waves

contribute to interaction. The former is termed the three-wave solution, and the latter, the four-wave solution.

A. THREE-WAVE SOLUTION

Consider a circuit of length L, in which the number of electron wavelengths measured along the circuit, N_e, is

$$N_e = \frac{\beta_e L}{2\pi} \qquad \text{or} \qquad L = \frac{2\pi N_e}{\beta_e} .$$

Therefore at $z = L$, we have

$$e^{-\Gamma L} = \exp\left[j2\pi N_e \left(\frac{q\dot{\phi}_0}{\omega} - 1\right)\right] e^{\theta\delta}$$

where $\theta \triangleq 2\pi C N_e$. Therefore, the total E_ϕ-field at $z = L$ is the sum of three waves:

$$E_\phi(N_e) = \exp\left[j2\pi N_e \left(\frac{q\dot{\phi}_0}{\omega} - 1\right)\right]\left[E_{\phi 1}\, e^{\theta\delta_1} + E_{\phi 2}\, e^{\theta\delta_2} + E_{\phi 3}\, e^{\theta\delta_3}\right] , \quad (10)$$

where $E_{\phi 1}$ = amplitude of the wave associated with δ_1, etc., and where we have assumed that δ_4 corresponds to the forward wave.

For start oscillation we demand $E_\phi(N_e) = 0$, which is a homogeneous equation giving one relationship between the wave amplitudes. At $z = 0$, i.e., at the entrance to the circuit, there is no rf current, no rf velocity, and no rf displacement. As a result, we obtain two other homogeneous equations between the wave amplitudes. These homogeneous equations will have common solutions only when the determinant of their coefficients is zero, that is, only when

$$\begin{vmatrix} e^{\theta\delta_1} & e^{\theta\delta_2} & e^{\theta\delta_3} \\ \dfrac{G\Gamma_1 + H\delta_1}{\delta_1^2} & \dfrac{G\Gamma_2 + H\delta_2}{\delta_2^2} & \dfrac{G\Gamma_3 + H\delta_3}{\delta_3^2} \\ \dfrac{1}{\delta_1} & \dfrac{1}{\delta_2} & \dfrac{1}{\delta_3} \end{vmatrix} = 0 , \quad (11)$$

where $G \triangleq [(r_0\dot{\phi}_0)/c](\zeta/\omega C)$, $H \triangleq 1/(r_0\dot{\phi}_0)$.

The four δ's have already been solved for various b's in the solution of propagation constants; they are now tested, and the one corresponding to a forward wave is discarded. The remaining three δ's for each b are substituted into the left-hand side of Eq. (11) with θ varied to give the LHS = 0 . The entire calculation is done using a Burroughs 220. The results are plotted against frequency in Figs. 3-5. Figure 3 is that of b vs f . Figure 4 shows the three δ's vs f , and Fig. 5 shows the CN_e vs f as obtained from Eq. (11). In Fig. 5 three other results are plotted for comparison: the experimentally measured CN_e and two results of four-wave solutions. The experimental curve is obtained by assuming an L = 8-1/2" (i.e., length of the uniform magnetic field region). The CN_e's obtained from the three-wave solution do not agree well with the experimental results, expecially at the low frequency end. This is to be expected since at the low frequency end the reflections, which give rise to forward interference, become important. Therefore, for a self-consistent result, as indicated by one of the four-wave solutions, we must take into account the forward wave; this analysis will be presented next. It is interesting to note that with the three-wave solution, CN_e remains roughly constant at .34, agreeing well with the three-wave solution obtained by Johnson[7] (.314) for the conventional backward-wave oscillators using the three-wave solution. The values of b obtained are almost constant at 2, which differs slightly from that obtained by Johnson[7] (1.522).

B. FOUR-WAVE SOLUTION

In considering the four-wave solution, we shall add the forward-wave amplitude $E_{\phi 4}$ in all the equations discussed above. We have, however, to add another condition to the waves in order to solve them. This is connected with the reflection coefficient from the gun-end ρ , as was derived by Israelsen:[3]

$$\frac{\partial}{\partial z}\left(E_{\phi}\right)\Big|_{z=0} = j\beta\left(\frac{1-\rho}{1+\rho}\right)E_{\phi}(0) \ .$$

It should be noted that the ρ here is not the measured cold reflection coefficient, because it involves four waves with different propagation constants. Now for the four homogeneous boundary equations to have

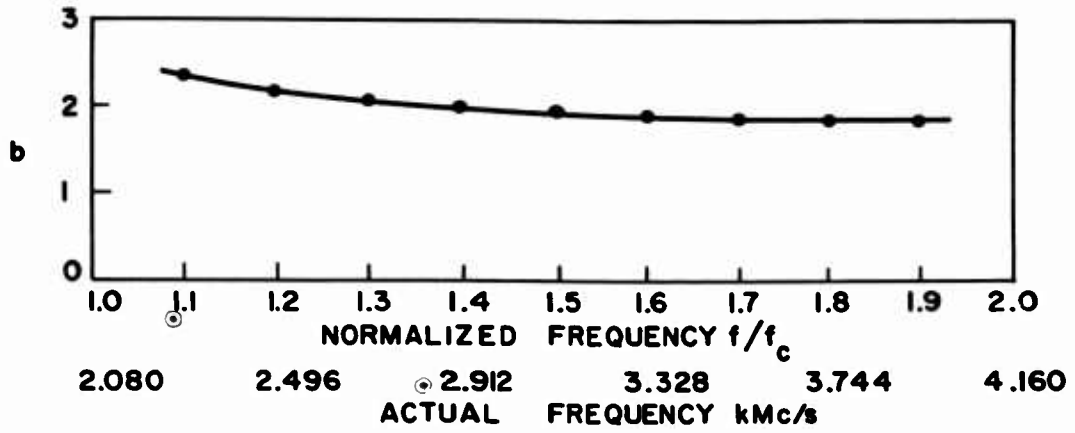

FIG. 3--Variation of b with f/f_c for three-wave solution, where f_c = cut off frequency of the dominant waveguide mode.

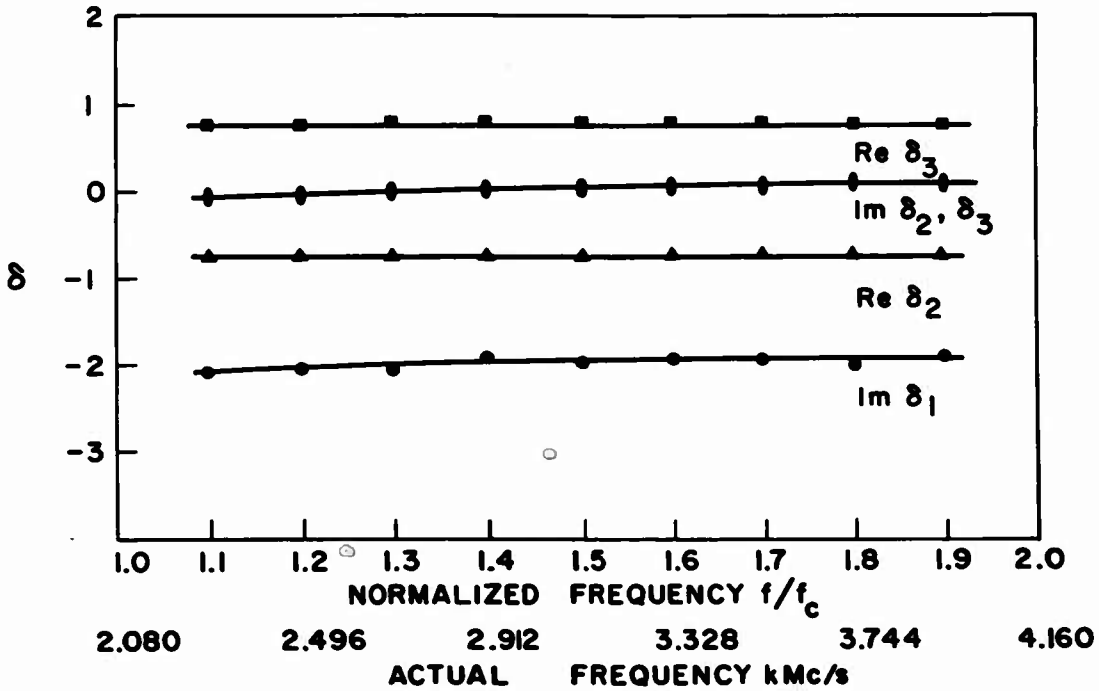

FIG. 4--Variation of δ's with f/f_c for three-wave solution. The δ's correspond to the three backward waves.

common solutions, we demand that

$$\begin{vmatrix} e^{\theta\delta_1} & e^{\theta\delta_2} & e^{\theta\delta_3} & e^{\theta\delta_4} \\ \dfrac{G\Gamma_1 + H\delta_1}{\delta_1^2} & \dfrac{G\Gamma_2 + H\delta_2}{\delta_2^2} & \dfrac{G\Gamma_3 + H\delta_3}{\delta_3^2} & \dfrac{G\Gamma_4 + H\delta_4}{\delta_4^2} \\ \dfrac{1}{\delta_1} & \dfrac{1}{\delta_2} & \dfrac{1}{\delta_3} & \dfrac{1}{\delta_4} \\ js + \delta_1 & js + \delta_2 & js + \delta_3 & js + \delta_4 \end{vmatrix} = 0 , \qquad (12)$$

where

$$s = \frac{\rho}{(\beta_e C/2\beta)(1 + \rho)} + b .$$

The determinantal equation (12) is again solved using the Burroughs 220 computer as follows: the δ's are calculated with various b's and then, by assuming values for θ and ρ, the left-hand side of Eq. (12) is calculated until it is equal to zero. The results are very interesting and are plotted in Figs. 5 and 6. Throughout the band, if ρ is assumed to be zero, the values of CN_e and b obtained for oscillation are virtually the same as those of the three-wave solution. This is to be expected because the forward wave will have very small amplitude at $\rho = 0$. If at the lower end, ρ is assumed to be unity at a phase angle varying between 0 and 45°, the CN_e's agree well with the experimental results (.15) with $b \approx 3.8$. At mid-band, with ρ equal to unity at phase angles varying from 90° to 180°, CN_e varies from .235 to .262, again agreeing well with the experimental result; in this case b varies from 4.1 to 3.9. At the high frequency end, however, ρ equal to 1 gives excellent agreement, and $\rho = 0$, as mentioned before, gives good agreement.

It is interesting to note that, at the low frequency end, the CN_e obtained from the three-wave solution (or four-wave solution with $\rho \to 0$) is over twice that obtained from the four-wave solution with $\rho \to 1$. This corresponds to almost a factor of 10 in the starting currents, since $C \sim (I_0)^{1/3}$. By decreasing the reflections from the gun end, one should

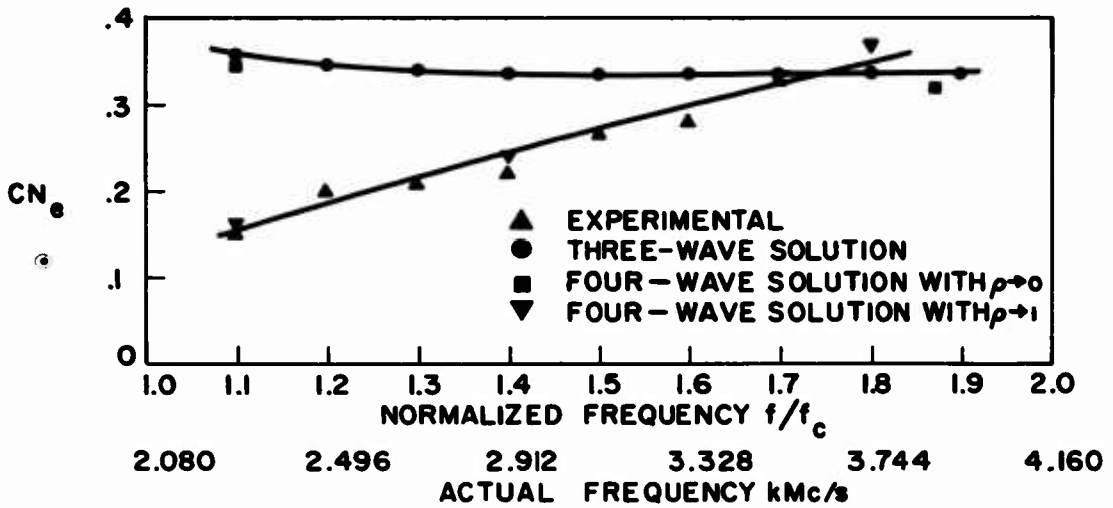

FIG. 5--Variation of experimentally measured and theoretically calculated CN_e with f/f_c .

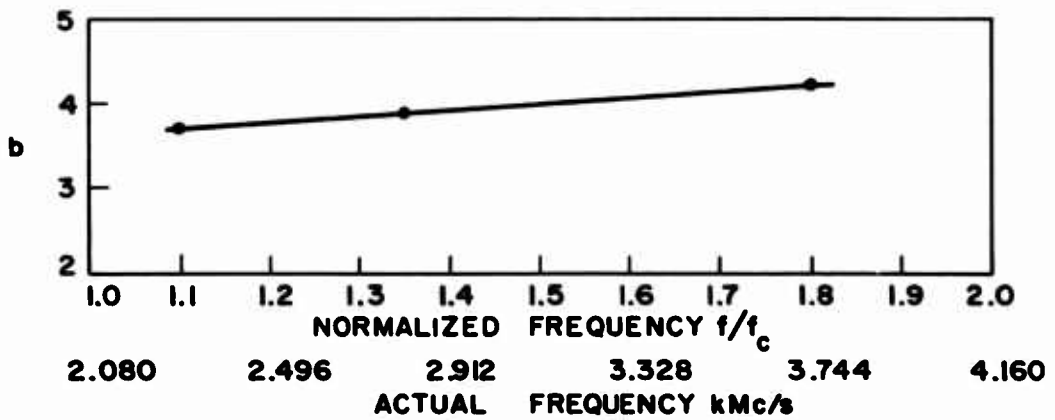

FIG. 6--Variation of b with f/f_c for four-wave solution, with $\rho \to 1$.

observe the increase of start-oscillation current, a result yet to be verified.

Thus, we can make the following general statements. From low frequency end to mid-band, tuning for best oscillation of the tube gives high reflection from the gun end (~ 1), for the forward-wave interference is important. From there on, the reflection is less and the forward wave is unimportant; hence, both $\rho = 1$ and $\rho = 0$ give good agreement. The start-oscillation current as given by the three-wave solution and the four-wave solution with $\rho = 0$ corresponds to the case where the rf H-field bunching is dominant, whereas that given by the four-wave solution with $\rho = 1$ corresponds to the participation of other interactions at the low-frequency end as given by the first term of Eq. (7).

In all the rf analysis above, no rf space-charge field is assumed. The rf space-charge forces were found to be unimportant because the theoretical results agree well with the experimental ones. This can be understood physically: there are many electron helices in parallel; the rf space-charge forces in one helix tend to be balanced out by the others so that the beam, as a whole, has no net rf space-charge field.

The existence of b indicates that interaction takes place not at the "exact dc synchronism," but at a value different from it. This beam slippage is necessary as explained by Pierce and Field[8] in dealing with TWT's.

The backward-wave gain can be computed similarly to the calculation of the start oscillation, since backward-wave gain is defined as the magnitude of the ratio of the E-field at the gun end to that at the other end of the circuit. This can be calculated by using the values of δ's and θ for current just under start oscillation, and by using values of ρ near that of start oscillation. The calculations are complicated, and can best be done by computer. Since the tube had very limited use as an amplifier, the calculations are not pursued.

VI. CONCLUSIONS

In conclusion, the analysis has shown excellent agreement with the experimental results, and has confirmed many predictions made from physical arguments. Of particular interest are the facts that (1) the electron

bunching and energy extraction mechanisms are fundamentally different from those in O-type tubes, (ii) the start-oscillation current is much dependent on reflection from the gun end, and (iii) the rf space-charge forces are unimportant. The other behaviors of the tube as an amplifier and as an oscillator can be easily understood by referring to the Brillouin diagram.

For higher frequency operation by scaling the S-band tube, the dc magnetic field has to increase linearly with frequency, for interaction with higher harmonics is inefficient using this circuit geometry.

REFERENCES

1. K. K. Chow and R. H. Pantell, "The Cyclotron Resonance Backward-Wave Oscillator," Proc. IRE, Vol. 48, pp. 1865-1870 (November 1960).
2. R. H. Pantell, "Small-Signal Analysis of the Helitron Oscillator," IRE Trans. PGED, Vol. ED-7, No. 1, pp. 22-29 (January 1960).
3. B. P. Israelsen, "Investigation of the Helitron Oscillator," Technical Report No. 404-1, Electron Device Laboratory, Stanford Electronics Laboratories, Stanford University, Stanford, California (November 1959).
4. K. K. Chow, "The Cyclotron-Resonance Oscillator," Microwave Laboratory Report No. 800, Stanford University, Stanford, California (April 1961).
5. D. L. Bobroff, "Independent Space Variables for Small-Signal Electron-Beam Analysis," IRE Trans PGED, Vol. ED-6, No. 1, pp. 68-78 (January 1959).
6. J. R. Pierce, Traveling-Wave Tubes, (D. Van Nostrand Company, Inc., New York, 1950).
7. H. R. Johnson, "Backward-Wave Oscillators," Proc. IRE, Vol. 43, pp. 684-687 (June 1955).
8. J. R. Pierce and L. M. Field, "Traveling-Wave Tubes," Proc. IRE, Vol. 35, pp. 108-111 (February 1947).

DISTRIBUTION LIST

ASTIA (10)
Arlington Hall Station
Arlington, Virginia

Bell Telephone Laboratories
Murray Hill Laboratory
Murray Hill, New Jersey
Attention: Dr. J. R. Pierce

Lt. Col. W. B. Lindsay
Adv. Res. Projects Agency
Washington 25, D. C.

California Institute of Technology
Department of Electrical Engineering
Pasadena, California
Attention: Prof. L. M. Field

National Science Foundation (5)
1951 Constitution Ave., N. W.
Washington 25, D. C.

Dr. A. H. W. Beck
Engineering Laboratory
Cambridge University
Cambridge, Trumpington Street
England

Professor G. B. Walker
University of British Columbia
Vancouver 8, B. C.
Canada

Ohio State University
Department of Electrical Engineering
Columbus 10, Ohio
Attention: Prof. E. M. Boone

Director
Electronics Defense Group
Engineering Research Institute
University of Michigan
Ann Arbor, Michigan

Johns Hopkins University
Radiation Laboratory
1315 St. Paul Street
Baltimore 2, Maryland
Attention: Dr. D. D. King

Columbia University
Columbia Radiation Laboratory
New York 27, New York
Attention: Mr. Bernstein

Cruft Laboratory
Harvard University
Cambridge, Massachusetts

Dr. Winston H. Bostick
Department of Physics
Stevens Institute of Technology
Hoboken, New Jersey

University of Michigan
Willow Run Research Center
Engineering Research Institute
Ann Arbor, Michigan
Attention: Dr. H. Goode

Massachusetts Institute of Technology
Research Laboratory of Electronics
Cambridge 39, Massachusetts
Attention: Mr. Hewitt (Librarian)

Brooklyn Polytechnic Institute
Microwave Research Institute
55 Johnson Street
Brooklyn 1, New York
Attention: Mr. Jerome Fox

Dr. Paul D. Coleman
Electrical Engineering Department
Control Systems Laboratory
University of Illinois
Urbana, Illinois

Dr. John R. Whinnery
Division of Electrical Engineering
University of California
Berkeley 4, California

Professor Hans Motz
Oxford University
Oxford, England

Lincoln Laboratory
Massachusetts Institute of Technology
P. O. Box 73
Lexington, Massachusetts

Mr. Paul C. Yuen
Research Engineer
Electronics Research Laboratory
Illinois Institute of Technology
Technology Center
Chicago 16, Illinois

Dr. Tore Wessel-Berg
Norwegian Defense Research
Establishment
Radar Division
Bergen, Norway

Dr. A. F. Pearch
Imperial College of Science
and Technology
South Kensington
London, W., England

Stanford Research Institute
Menlo Park, California
Attention: Document Center

California Institute of Technology
Electron Tube Laboratory
Pasadena, California
Attention: Prof. R. W. Gould

Radio Research Laboratories
Kokubunji, P. O.
Tokyo, Japan

University of Southern California
University Park
Los Angeles 7, California
Attention: Z. A. Kaprielian, Assoc.
Prof. of Electrical
Engineering

Dr. A. L. Cullen
Department of Electrical Engineering
University of Sheffield
Sheffield 1, England

Advisory Group on Electron Tubes
346 Broadway, 8th Floor
New York 13, New York
Attention: Secretary, Working Group
on Semiconductor Devices

Bell Telephone Laboratories, Inc.
Whippany Laboratory
Whippany, New Jersey
Attention: Technical Information
Library

Hughes Aircraft Company
Florence Avenue and Teale Street
Culver City, California
Attention: Documents Section,
Research and Development
Library

General Electric Company
Microwave Laboratory
601 South California Avenue
Palo Alto, California
Attention: Librarian

Sylvania Electric Products, Inc.
Electronic Defense Laboratory
P. O. Box 205
Mountain View, California
Attention: Library

Boston Sub Office
Patent Prosecution Branch (Hq. AMC)
Murphy General Hospital, Bldg. 133
424 Trapelo Road
Waltham 54, Massachusetts

Office of Technical Services
Department of Commerce
Washington 25, D. C.
Attention: Technical Reports Section

Library
Boulder Laboratories
National Bureau of Standards
Boulder, Colorado

Institute of the Aeronautical Sciences
2 East 64th Street
New York 21, New York
Attention: Librarian

Sperry Gyroscope Company
Division of Sperry Rand Corporation
Great Neck, New York
Attention: Mrs. Florence W. Turnbull

General Telephone and Electronics
Laboratories, Inc.
Bayside, New York
Attention: Mr. D. Lazare, Manager
Technical Services

Professor Richard W. Grow
Electrical Engineering Department
University of Utah
Salt Lake City, Utah

Varian Associates
611 Hansen Way
Palo Alto, California
Attention: Mr. W. J. Dodds

Standard Telephone Laboratories
Harlow, Essex, England
Attention: Dr. E. A. Ash

University of Chicago
Midway Laboratories
6220 S. Drexel Avenue
Chicago, Illinois
Attention: P. J. Dickerman

General Electric Company
P. O. Box 1088
Schenectady, New York
Attention: Mr. E. D. McArthur
Research Laboratories

Dr. J. T. Senise
Instituto Tecnológico de Aeronáutica
São José dos Campos
São Paulo, Brazil

UNCLASSIFIED